IIE Transactions (2013) **45**, 1235–1247

ISSN: 0740-817X print / 1545-8830 online
DOI: 10.1080/0740817X.2013.770187

Monitoring and diagnosis of multichannel nonlinear profile variations using uncorrelated multilinear principal component analysis

KAMRAN PAYNABAR[1], JIONGHUA (JUDY) JIN[2,*] and MASSIMO PACELLA[3]

[1]*H. Milton Stewart School of Industrial & Systems Engineering, Georgia Institute of Technology, Atlanta, GA 30332-0205, USA*
[2]*Department of Industrial and Operations Engineering, University of Michigan, Ann Arbor, MI 48109-2117, USA*
E-mail: jhjin@umich.edu
[3]*Dipartimento di Ingegneria dell'Innovazione, Universita' del Salento, Piazza Tancredi 7, 73100 Lecce, Italy*

Received October 2011 and accepted September 2012

In modern manufacturing systems, online sensing is being increasingly used for process monitoring and fault diagnosis. In many practical situations, the output of the sensing system is represented by time-ordered data known as *profiles* or *waveform signals.* Most of the work reported in the literature has dealt with cases in which the production process is characterized by single profiles. In some industrial practices, however, the online sensing system is designed so that it records more than one profile at each operation cycle. For example, in multi-operation forging processes with transfer or progressive dies, four sensors are used to measure the tonnage force exerted on dies. To effectively analyze multichannel profiles, it is crucial to develop a method that considers the interrelationships between different profile channels. A method for analyzing multichannel profiles based on uncorrelated multilinear principal component analysis is proposed in this article for the purpose of characterizing process variations, fault detection, and fault diagnosis. The effectiveness of the proposed method is demonstrated by using simulations and a case study on a multi-operation forging process.

Keywords: Classification, dimension reduction, principal component analysis, tensor-to-vector projection

1. Introduction

Online sensing is being increasingly used for process monitoring and fault diagnosis in modern manufacturing systems. In many practical situations, the output of an automatic sensor is represented by spatial- or time-ordered data known as *profiles* or *waveform signals.* Examples of profile data include the roundness profile of a machined part measured at different sampling angles in a lathe-turning process (Colosimo *et al*., 2008; Moroni and Pacella, 2008) and the ram force signals used to press valve seats into engine heads in an engine head assembly process (Paynabar and Jin, 2011).

There is extensive research on modeling and monitoring of linear profiles reported in the literature. For example, see the work of Kang and Albin (2000), Kim *et al*. (2003), Mahmoud and Woodall (2004), Gupta *et al*. (2006), Zou *et al*. (2006), Mahmoud *et al*. (2007), and Jensen *et al*. (2008). However, in most practical situations, the output of a sensor is represented by a nonlinear profile. There is increasing research interest in developing effective techniques for process monitoring and fault diagnosis using nonlinear profile data. Gardner *et al*. (1997) and Walker and Wright (2002) utilized spline regression to model and analyze nonlinear profile data. For the purpose of monitoring and faults diagnosis, Jin and Shi (2001) proposed a classification scheme for nonlinear profiles using wavelets. Williams *et al*. (2007) used a four-parameter logistic regression and smoothing spline to model and monitor the dose–response profiles of a drug. Paynabar *et al*. (2012) used a nonlinear parametric regression model to develop a robust leak-testing procedure for transmission systems. To monitor nonlinear profiles in Phase I, Ding *et al*. (2006) considered each profile as high-dimensional data and applied Principal Component Analysis (PCA) and independent component analysis to reduce the dimensions of the nonlinear profiles. For the purpose of dimension reduction, Jung *et al*. (2006a, 2006b) proposed wavelet-based threshold methods based on multiple samples of profiles collected from a single sensor. They also employed the extracted wavelet features to detect different types of faults in a process. Zou *et al*. (2008) applied local linear smoothers to monitor nonlinear profiles. Zou *et al*. (2009) applied the

*Corresponding author

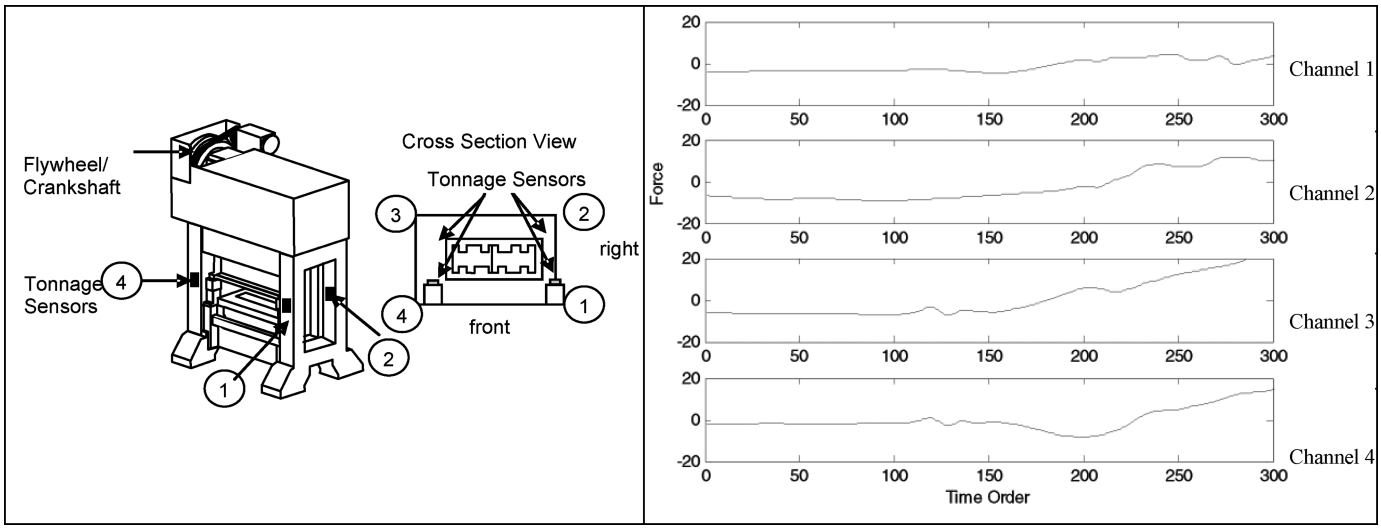

Fig. 1. Forging process generating multichannel signal data: (a) (left panel): A forging machine with four strain gauges and (b) (right panel): a sample of four-channel profiles.

generalized likelihood ratio test to develop a monitoring procedure for nonlinear profiles modeled by local linear kernel smoothing. Furthermore, in order to account for profile-to-profile variations in profile modeling and monitoring, Mosesova *et al*. (2006) and Jensen and Birch (2009) used nonlinear parametric mixed-effect regression. Paynabar and Jin (2011) further addressed this problem by developing a wavelet-based mixed-effect model for modeling nonlinear profiles and characterizing the profile variations. To monitor nonlinear profiles, Qiu *et al*. (2010) developed mixed-effect models based on kernel regression.

Most of the work reported in the literature dealt with cases in which the underlying process performance was reflected by individual profiles. In some industrial processes, however, multiple sensors have to be used to capture the overall system responses. For example, in multi-operation forging processes with transfer or progressive dies, in order to measure the total press tonnage force exerted on all dies, multiple sensors are used. As shown in Fig. 1(a), four strain gauge sensors are installed on the four uprights of a forging press, and each sensor records the tonnage force profile at the predefined equal sampling interval of a rotational crank angle. In Fig. 1(b), one sample of partial tonnage profiles corresponding to each sensor during a press stroke is depicted against the sampling data index. Since such multiple profiles are recorded through different sensor channels, they are called *multichannel profiles* in this article.

The topic of data fusion for application in process monitoring applications and fault diagnosis studies using multisensor data have been extensively studied in literature. For example, Gao and Durrant-Whyte (1994), Basir and Yuan (2007), Mosallaei *et al*. (2007), and Quan *et al*. (2010), among others, have proposed different methods for sensor fusion with application to fault diagnosis. However, the sensor data structure used in those articles is different from that used in this article. In this article, each profile signal is represented as a vector of data points measured by each sensor (channel) during each repetitive operating cycle; i.e., each sample of p-channel profile signals contains p vectors of profile data. In contrast, in the discussed articles, each sample of p-sensor data includes p scalar observations; i.e., each sensor has one single data point. Therefore, the techniques and methods presented in the existing literature cannot be simply applied to our data. There is little research in the literature on analyzing multichannel profile data. In most existing research, multichannel profiles were represented as one aggregated tonnage profile through adding up all channels' signals (see, for example, the work by Kim *et al*. (2006) and Lei *et al*. (2010)). Although the aggregated tonnage profile represents the total tonnage force, some valuable cross-correlation information among channels is lost due to the aggregation of all the channels. An alternative approach for dealing with multichannel profiles is to analyze each profile individually. This approach, again, fails to consider the interrelationship among the multichannel profiles. For example, as will be discussed later in the case study section, the interrelationship among the four channels' monitoring tonnage profiles can provide useful diagnostic information about process faults. However, such information cannot be captured if profiles are analyzed one at a time. Therefore, the objective of this article is to develop an effective method that can analyze multichannel profiles by considering the interrelationship among all channels simultaneously.

PCA has been widely used as an effective tool for dimension reduction and variation characterization of nonlinear profiles. However, regular PCA cannot be directly applied to multichannel profiles since there are four profile channels in each data sample. One approach to overcome this

issue is to combine multichannel profiles and turn them into one high-dimensional vector. For example, a sample of p-channel sensing signals with each channel signal of size m would turn into a vector of size $mp \times 1$. Henceforth, this method is referred to as Vectorized-PCA (VPCA). Although VPCA has been used in different applications such as image processing applications (see, for example, Bharati and MacGregor (1998) and Bharati *et al*. (2004)), there are several issues in using VPCA for tensor data such as multichannel profiles. The computational complexity and memory demands of VPCA are higher than regular PCA since the dimension of the covariance matrix significantly increases due to the increase of data dimensions induced by vectoriziation. Moreover, this approach breaks the correlation structure in the original data and loses potentially more compact or useful representations that can be obtained in the original form (Ye *et al*., 2004). Lu *et al*. (2008) introduced the Multilinear PCA (MPCA) formulation as an alternative to VPCA. MPCA is a multilinear dimensionality reduction and feature extraction method. This method operates directly on the multi-dimensional data rather than on the vectorized version of them; hence, MPCA is naturally applicable to data with the matrix or higher-order tensor representation. The principal components obtained from MPCA, however, are correlated contrary to regular PCA. To overcome this issue, Lu *et al*. (2009) proposed Uncorrelated MPCA (UMPCA). In this method, in addition to the tensor-to-vector projection used in MPCA, a zero-correlation constraint is enforced on the produced features. Although there is some exploratory research on the applications of UMPCA to image processing and computer vision (Lu *et al*., 2009), very little research could be found in the literature on using the UMPCA technique for analyzing multichannel nonlinear profiles for the purpose of fault detection and diagnosis. Unlike VPCA, UMPCA does not break the tensor structure of multichannel profile data and hence can preserve potentially more compact and useful interpretations than those that can be obtained in the vectorized representation form of VPCA. Furthermore, as will be shown in both simulations and the case study, in VPCA, if there is any large variation pattern in one of the profile channels, this variation may affect multiple eigenvectors, which can mask the variation patterns and delude the interrelationship of other channels. However, this issue does not occur in UMPCA as it directly works with tensor data. It is known that analyzing multichannel nonlinear profiles is much more challenging than analyzing single-channel profiles because of the additional complexity due to the interrelationship among multiple channels. Therefore, the main goal of this article is to propose a UMPCA-based approach for analyzing multichannel profiles that considers the interrelationship of different profile channels. The proposed approach provides a set of extracted features that can be effectively used to characterize process variations and fault diagnosis. The effectiveness of the proposed method is shown via both Monte Carlo simulations and a real-world case study in a multi-operation forging process.

The rest of this article is organized as follows. In Section 2, the method for analysis and dimension reduction of multichannel nonlinear profiles using UMPCA is presented. VPCA is also reviewed in this section. In Section 3, using Monte Carlo simulations, the performance of UMPCA and VPCA in modeling and characterizing the variations of multichannel profiles are evaluated and compared. Section 4 is devoted to a real case study of a multi-operation forging process. In this section, the proposed method is applied to multichannel nonlinear tonnage profiles for the purpose of variation characterization and fault diagnosis. Finally, the article is concluded in Section 5.

2. Dimension reduction of multichannel profiles using UMPCA and VPCA

In this section, the implementation of UMPCA and VPCA for the purpose of dimensionality reduction in multichannel nonlinear profiles is presented. The basic concepts of the multilinear algebra used in UMPCA are also reviewed. Readers interested in the theory behind the mathematical development of UMPCA based on multilinear singular value decomposition are referred to Lathauwer *et al*. (2000a, 2000b) and Kolda (2001). The algorithm we use in this article for extracting uncorrelated features from tensor data is based on the theories presented in those articles.

2.1. *Basic notations and definitions*

Consider a set of n samples (sample index $k = 1, 2, \ldots, n$) of p-channel profile (sensor or channel index $j = 1, 2, \ldots, p$), in which each channel sensing profile consists of m measured values (data index $i = 1, 2, \ldots, m$). Therefore, the kth sample of multichannel signals can be represented by matrix $\mathbf{V}_k(i, j) \in \Re^{m \times p}$. In multilinear algebra, a matrix can be considered to be a second-order tensor. A dth-order tensor in multidimensional space is a d-dimensional vector with d indices and $\prod_{r=1}^{d} t_r$ components, where t_r is the length of the vector in the dth dimension. Each index of a tensor corresponds to one dimension of space (Lu *et al*., 2008). Generally speaking, tensors are generalizations of matrices in three- or higher-dimensional space. By definition, the l-mode vector of $\mathbf{V}_k(i, j)$ is defined as the vector obtained by varying the lth index in (i, j) while keeping all other indexes fixed; i.e., each row vector and column vector can be generally called the l-mode vector ($l = 1, 2$) of $\mathbf{V}_k(i, j)$. Therefore, the 1-mode vectors of $\mathbf{V}_k(i, j)$ are m-dimensional vectors represent the jth channel sensing signal (i.e., the jth column vector of $\mathbf{V}_k(i, j)$) of sample k and are obtained by varying the first index i ($i = 1, \ldots, m$) and fixing the second index j. The 2-mode vectors of $\mathbf{V}_k(i, j)$ are the p-dimensional

vectors that represent ith row vector of $\mathbf{V}_k(i, j)$ of sample k and are obtained by varying the second index j and fixing the first index i. That is, the elements of the kth 2-mode vector correspond to the data measured by all sensors at measurement index j of sample k. Furthermore, the l-mode ($l = 1, \ldots, d$) product of the tensor $\mathbf{S} \in \Re^{I_1 \times I_2 \times \cdots I_d}$ by matrix $\mathbf{U} \in \Re^{J_l \times I_l}$ denoted by $\mathbf{S} \times_l \mathbf{U}$ is obtained by $(\mathbf{S} \times_l \mathbf{U})(i_1, i_2, \ldots, i_{l-1}, j_l, i_{l+1}, \ldots, i_d) = \sum_{i_l=1}^{I_l} \mathbf{S}(i_1, i_2, \ldots, i_l, \ldots, i_d)\mathbf{U}(j_l, i_l)$. The scalar product of two matrices $\mathbf{A}, \mathbf{B} \in \Re^{I_1 \times I_2}$ is defined as $\langle \mathbf{A}, \mathbf{B} \rangle = \sum_{i_1} \sum_{i_2} \mathbf{A}(i_1, i_2)\mathbf{B}(i_1, i_2)$. Another useful operation is the Tensor-to-Vector Projection (TVP). A TVP consists of multiple Elementary Multilinear Projections (EMPs), which are composed of unit projection vector per mode (Lu *et al*., 2009). An EMP projects a tensor to a scalar. For example, let $\{\mathbf{u}^{(1)^{\mathrm{T}}}, \mathbf{u}^{(2)^{\mathrm{T}}}\}$ with $\|\mathbf{u}^{(l)}\| = 1$ be an EMP for matrix $\mathbf{V}_k$, where $\|\|$ denotes the Euclidean norm and superscript T indicates the transpose operation. The EMP projects matrix $\mathbf{V}_k$ to a scalar y denoted by $y = \mathbf{V}_k \times_{l=1}^{2} \{\mathbf{u}^{(1)^{\mathrm{T}}}, \mathbf{u}^{(2)^{\mathrm{T}}}\} = \mathbf{V}_k \times_1 \mathbf{u}^{(1)^{\mathrm{T}}} \times_2 \mathbf{u}^{(2)^{\mathrm{T}}} = \langle \mathbf{V}_k, \mathbf{U} \rangle$, where $\mathbf{U}$ is the outer product of $\mathbf{u}^{(1)}$ and $\mathbf{u}^{(2)}$ denoted by $\mathbf{U} = \mathbf{u}^{(1)} \circ \mathbf{u}^{(2)}$. Suppose there are R available EMPs for matrix $\mathbf{V}_k$ which can be represented as $\{\mathbf{u}_r^{(1)^{\mathrm{T}}}, \mathbf{u}_r^{(2)^{\mathrm{T}}}\}_{r=1}^{R}$. In this case, the TVP of matrix $\mathbf{V}_k$ to a vector $\mathbf{y}$ can be obtained by $\mathbf{y} = \mathbf{V}_k \times_{l=1}^{2} \{\mathbf{u}_r^{(l)^{\mathrm{T}}}\}_{r=1}^{R}$, where the rth element of vector $\mathbf{y}$ is $\mathbf{y}(r) = \mathbf{V}_k \times_1 \mathbf{u}_r^{(1)^{\mathrm{T}}} \times_2 \mathbf{u}_r^{(2)^{\mathrm{T}}}$. The basis tensors $\times_{l=1}^{2} \{\mathbf{u}_r^{(l)^{\mathrm{T}}}\}_{r=1}^{R}$ are called eigentensors in the literature (Lu *et al*., 2009).

2.2. *Uncorrelated MPCA*

Recently, there has been an increasing research interest in generalizing PCA to tensor objects without changing the structure of the tensor. MPCA, introduced by Lu *et al*. (2008), is a multilinear dimensionality reduction and feature extraction method, which can be applied to tensors. The projected tensors obtained from MPCA, however, are correlated contrary to regular PCA. To overcome this issue, Lu *et al*. (2009) proposed UMPCA, in which a TVP projection is used for projection. In this subsection we review the UMPCA method proposed by Lu *et al*. (2009).

The derivation of the UMPCA algorithm follows the classic PCA derivation of successive variance maximization (Jolliffe, 2002). A number of elementary multilinear projections are solved one by one to maximize the captured variance with an enforced zero-correlation constraint. To formulate the UMPCA problem, let $\{\mathbf{y}_k(r); k = 1, 2, \ldots, n\}$ denote the set of rth principal components for all signal samples, where $\mathbf{y}_k(r) = \mathbf{V}_k \times_{l=1}^{2} \{\mathbf{u}_r^{(l)^{\mathrm{T}}}\}_{r=1}^{R}$ is the projection of the kth sample using the rth EMP. Let $\{\mathbf{g}_r \in \Re^m; r = 1, 2, \ldots, R\}$ denote the set of coordinate vectors. Therefore, the kth projected sample signal using the rth EMP is equivalent to the kth element of the rth coordinate vector; i.e., $\mathbf{y}_k(r) = \mathbf{g}_r(k)$. Accordingly, the total scatter of the transformed profiles denoted by S_r can be obtained by

$$S_r = \sum_{k=1}^{n} (\mathbf{y}_k(r) - \bar{y}_r)^2, \tag{1}$$

where $\bar{y}_r$ is the sample mean of projected profiles using the rth EMP. The UMPCA seeks a set of EMPs to maximize the variance of projected profiles in each EMP, while the obtained principal components are uncorrelated. The mathematical formulation of UMPCA can be written as

$$\left\{\mathbf{u}_r^{(l)^{\mathrm{T}}}, l = 1, 2\right\} = \arg\max_{\mathbf{u}_r^{(l)^{\mathrm{T}}}} S_r \quad \text{subject to} \begin{cases} \mathbf{u}_r^{(l)^{\mathrm{T}}}\mathbf{u}_r^{(l)} = 1 & \text{for all } r = 1, 2, \ldots, R \\ \mathbf{g}_r^{\mathrm{T}}\mathbf{g}_s = 0 & \text{for all } r \text{ and } s; r \neq s. \end{cases} \tag{2}$$

The EMP $\{\mathbf{u}_r^{(l)^{\mathrm{T}}}, l = 1, 2\}$ contains two sets of parameters, in which each set relates to one mode. To accurately obtain the rth EMP, it is necessary to determine $\mathbf{u}_r^{(1)}$ and $\mathbf{u}_r^{(2)}$ simultaneously such that the total scatter matrix of S_r is maximized. However, in multilinear algebra, there is no closed-form solution for this problem except for the case that we deal with one-channel profile ($R = 1$), in which the UMPCA boils down to the regular PCA. Therefore, an approximate iterative approach that considers one mode at a time is used to determine each EMP. This approach breaks down the problem to as many sub-problems as the number of modes and solves each sub-problem to determine $\mathbf{u}_r^{(l)}$ given the sets of vectors in the other mode. Detailed information about this approach can be found in Lu *et al*. (2008, 2009).

2.3. *VPCA*

VPCA is a generalization of PCA to tensor data, which applies the regular PCA to a tensor object reshaped into a vector. In the case of multichannel profiles, matrices $\mathbf{V}_k \in \Re^{m \times p}; k = 1, 2, \ldots, n$ can be reshaped into a vector $\mathbf{x}_k \in \Re^{mp \times 1}; k = 1, 2, \ldots, n$. Therefore, using this notation, all signal samples can be represented in a matrix form as $\mathbf{X} \in \Re^{n \times mp}; \mathbf{X} = [\mathbf{x}_1^{\mathrm{T}}, \mathbf{x}_2^{\mathrm{T}}, \ldots, \mathbf{x}_n^{\mathrm{T}}]^{\mathrm{T}}$. Then, the regular PCA is applied to matrix $\mathbf{X}$. Since signal data in $\mathbf{X}$ are centered, it suffices to solve the following decomposition problem:

$$\begin{cases} \mathbf{X}\mathbf{X}^{\mathrm{T}}\mathbf{e} = (n-1)\tau\mathbf{e} \\ \mathbf{e}^{\mathrm{T}}\mathbf{e} = 1 \end{cases}, \tag{3}$$

where $\mathbf{e}$ is an eigenvector and τ is an eigenvalue of the covariance matrix of $\mathbf{X}$. The eigenvectors corresponding to the w largest eigenvalues, denoted by $\mathbf{e}_q, q = 1, 2, \ldots, w$, are selected to form the transformation matrix $\mathbf{E}$, where w is the desired dimension of the transformed space. Hence, the transformed signal samples can be obtained by

$$\mathbf{Z} = \mathbf{X}\mathbf{E}, \tag{4}$$

where $\mathbf{Z} \in \Re^{n\times w}$ is the matrix of the transformed profile samples with each row representing one sample, and $\mathbf{E} \in \Re^{mp\times w}$; $\mathbf{E} = [\mathbf{e}_1, \mathbf{e}_2, \ldots, \mathbf{e}_w]$.

3. Performance comparison between UMPCA and VPCA using simulations

In this section, using Monte Carlo simulations, the performance of UMPCA and VPCA in characterizing the variations of multichannel profiles is evaluated and compared to each other. For this purpose, we consider a multioperation forging process with four strain gages to record four-channel pressing force signals (Lei *et al*., 2010). Suppose that in this process a four-channel profile ($p = 4$) is recorded at each cycle time and each profile consists of 175 ($m = 175$) data points. We generate 250 ($n = 250$) random profiles for each channel in this study. In order to investigate the effectiveness of UMPCA and VPCA in modeling the variations of multichannel profiles and interrelationship among them, two scenarios simulating two different variation patterns are studied. In the first scenario, the profile channels are randomly generated so that the variation magnitude is the same across all profile channels. In other words, in this scenario all profile channels have the same importance. In the second scenario, however, the variance of channels 1 and 2 is five times larger than the variance of other channels. That is, the variances of the first two channels are dominant. Furthermore, to include the interrelationship of profiles in both scenarios, profile channels 1 and 3 are considered to be correlated with profile channels 2 and 4, respectively. Conversely, profile channels 1 and 2 are considered to be independent of profile channels 3 and 4, respectively.

To simulate profile channels under the described scenarios, random effect (RE) models are used. Four RE models with B-spline basis are utilized to generate random nonlinear profile data for each scenario. In the RE model, there exists an RE corresponding to each model coefficient (Demidenko, 2004). The RE models used in simulations can be represented by

$$\mathbf{y}_i^{(k)} = \mathbf{X}^{(k)}\left(\boldsymbol{\beta}^{(k)} + \mathbf{b}_i^{(k)}\right) + \boldsymbol{\varepsilon}_i^{(k)},\ i = 1, 2, \ldots, n;\quad k = 1, 2, 3, 4, \tag{5}$$

where $\mathbf{y}_i^{(k)}$ is the $m \times 1$ vector of profile data for channel k, $\mathbf{X}$ is an $m \times t$ B-spline basis matrix of the regressor (time in our case); $\boldsymbol{\beta}^{(k)}$ is the $t \times 1$ vector of fixed-effects coefficients for profile channel k; $\mathbf{b}_i^{(k)} \sim \text{MVN}(0, \mathbf{D}^{(k)})$ is the $t \times 1$ vector of random effects coefficients for profile channel k, where $\mathbf{D}^{(k)}$ is a $t \times t$ diagonal positive definite matrix; and $\boldsymbol{\varepsilon}_i^{(k)} \sim \text{MVN}(0, \mathbf{I}\sigma_\varepsilon^2(k))$ is the $m \times 1$ vector of random noises for profile channel k, which is assumed to be independent of $\mathbf{b}_i^{(k)}$. Also, $\mathbf{I}^{(k)}$ is an $m \times m$ identity matrix, and $\sigma_\varepsilon^2(k)$ is the variance of random noises for profile channel k.

We used the sample average of a segment of tonnage profile data in the forging process, to be discussed in the next section, to determine the profile means in the RE model (5); i.e., $\mathbf{X}^{(k)}\boldsymbol{\beta}^{(k)}$. A B-spline basis with a degree of three is exploited as the fixed-effect basis. The matrix of fixed-effect coefficients used for simulation is

$$\mathbf{B} = \left[\boldsymbol{\beta}^{(1)}\boldsymbol{\beta}^{(2)}\boldsymbol{\beta}^{(3)}\boldsymbol{\beta}^{(4)}\right] = \begin{bmatrix} 111.22 & 87.15 & 108.94 & 105.93 \\ 122.65 & 104.72 & 112.85 & 123.41 \\ 159.15 & 122.40 & 145.49 & 143.20 \\ 192.60 & 159.30 & 159.03 & 160.75 \\ 166.48 & 137.45 & 154.08 & 146.87 \\ 144.58 & 127.45 & 137.08 & 128.37 \end{bmatrix}.$$

In scenario 1, $\text{var}(b_{ij}^{(1)}) = \text{var}(b_{ij}^{(2)}) = \text{var}(b_{ij}^{(3)}) = \text{var}(b_{ij}^{(4)}) = 10$, whereas in scenario 2, $\text{var}(b_{ij}^{(1)}) = \text{var}(b_{ij}^{(2)}) = 5\text{var}(b_{ij}^{(3)}) = 5\text{var}(b_{ij}^{(4)}) = 10$. In both scenarios, $\sigma_\varepsilon^2(k) = 1$, $\text{corr}(b_{ij}^{(1)}, b_{ij}^{(2)}) = -\text{corr}(b_{ij}^{(3)}, b_{ij}^{(4)}) = 0.9$, and other pairs of $\text{corr}(b_{ij}^{(k_1)}, b_{ij}^{(k_2)}) = 0; k_1 \neq k_2$, where $\text{corr}(a_1, a_2)$ represents the Pearson correlation coefficient of a_1 and a_2 and $b_{ij}^{(k_1)}; j = 1, 2, \ldots, m$ are the elements of $\mathbf{b}_i^{(k_1)}$. The overlapped nonlinear profile samples generated using scenario 2 are depicted in Fig. 2.

After generating profile samples, both UMPCA and VPCA were applied to the generated data using the procedures described in Section 2. In UMPCA, the eigentensors corresponding to the rth EMP, $\mathbf{U}_r \in \Re^{175\times 4}; r = 1, 2, 3, 4$, were obtained by $\mathbf{u}_r^{(1)} \circ \mathbf{u}_r^{(2)}$, where $\mathbf{u}^{(1)} \in \Re^{175\times 1}$ and $\mathbf{u}^{(2)} \in \Re^{4\times 1}$. Figure 3(a) shows $\mathbf{U}_r, r = 1, 2, 3, 4$, obtained from the generated profile data under scenario 1. Each column of $\mathbf{U}_r$ corresponds to one profile channel. The relative importance of the rth EMP denoted by c_r is defined as the ratio of the variance of transformed profiles using the rth EMP to the total variance of transformed profiles using all of the EMPs and calculated by $c_r = S_r / \sum_{r=1}^{4} S_r$. These values are 0.4901, 0.4572, 0.0314, and 0.0213 for the four EMPs, respectively. Based on the c_r values, the first two eigentensors are the most important eigentensors that are shown in Fig. 3(a). As can be seen from Fig. 3(a), the eigenvectors corresponding to the first EMP show a strong negative correlation between channels 3 and 4, whereas those corresponding to the second EMP indicate a strong positive correlation between channels 1 and 2 (eigenvectors of these channels are overlapped in the plot). The absolute correlation coefficients in both cases are larger than 0.95 with corresponding p-values less than 0.0001, which indicates significant correlation between the eigenvectors of channels 3 and 4 and channels 1 and 2. The relative importance values for the first and second EMP are close to each other, meaning that the variances of the profile channels are similar. These results are exactly compatible with the data

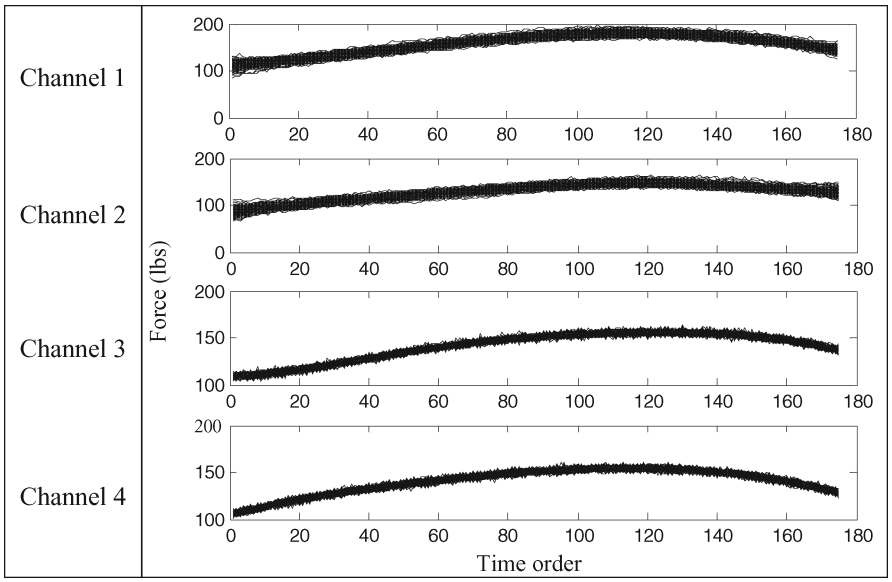

Fig. 2. Multichannel overlapped profile samples randomly generated under scenario 2.

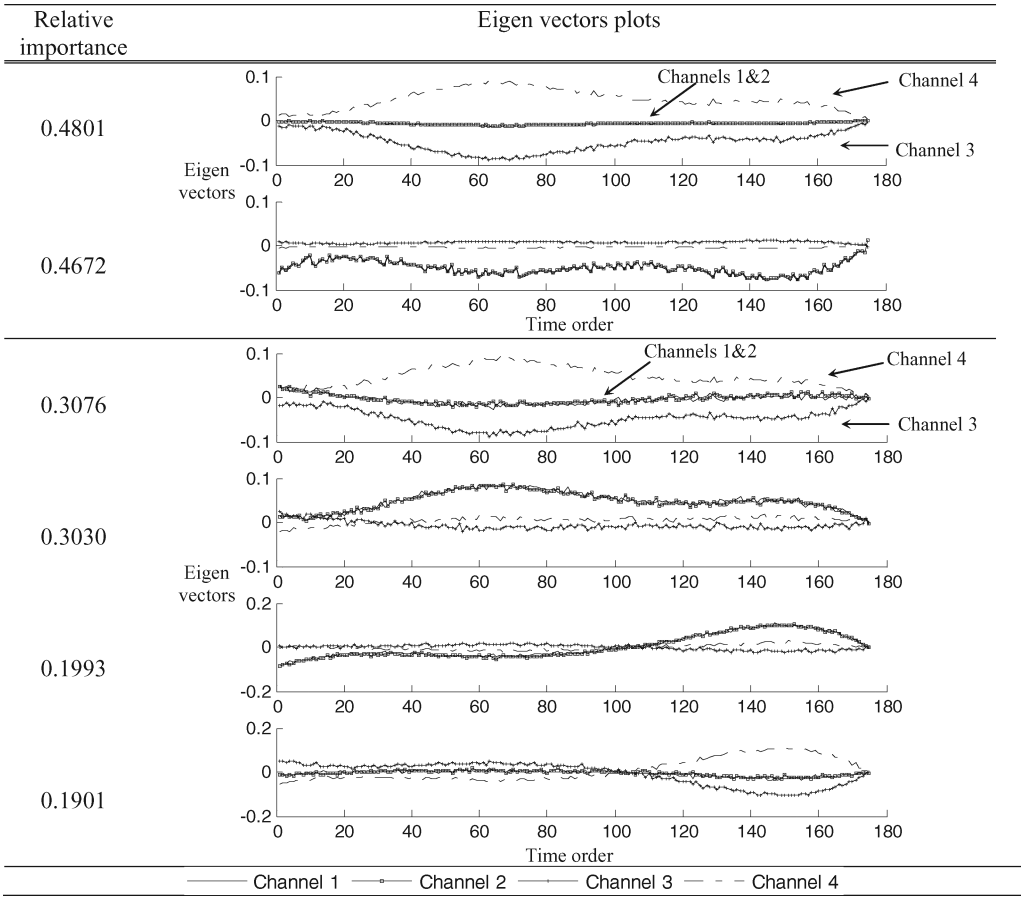

Fig. 3. UMPCA and VPCA results for simulation scenario 1: (a) (top panel) important eigentensors in UMPCA and (b) (bottom panel) important eigenvectors in VPCA.

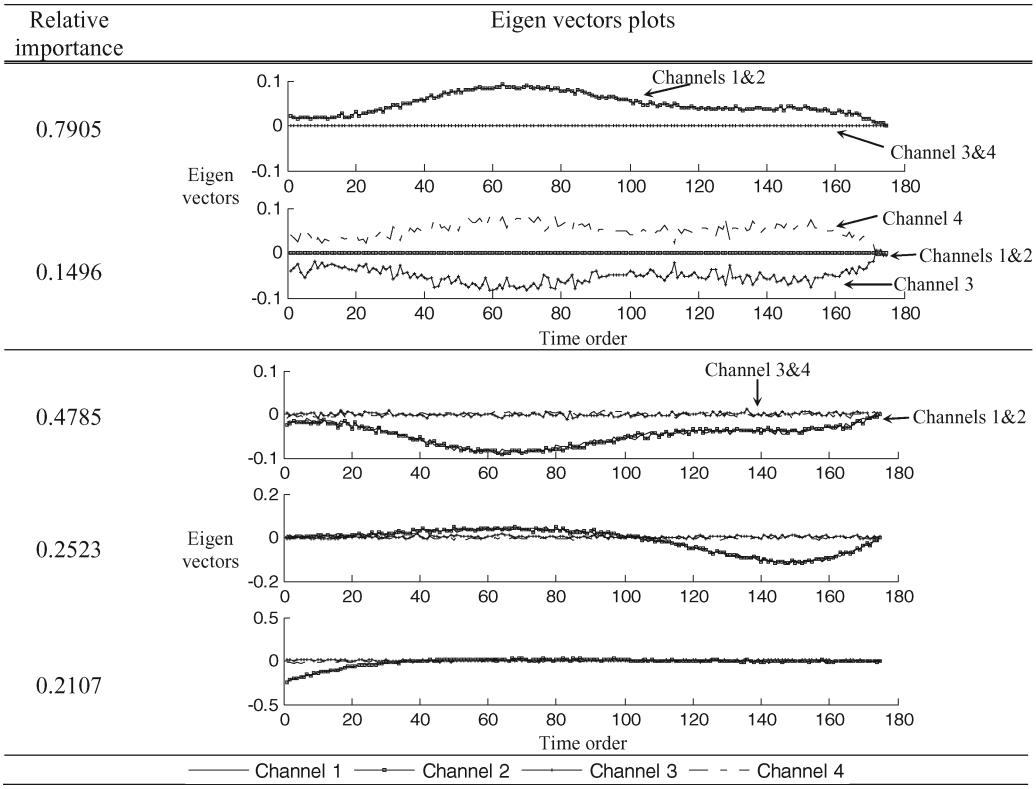

Fig. 4. UMPCA and VPCA results for simulation scenario 2: (a) (top panel): important eigentensors from UMPCA and (b) (bottom panel): important eigenvectors in VPCA.

generation model, thus implying that UMPCA can effectively extract information about multichannel profiles. Another interesting observation from Fig. 3(a) is that the eigenvectors of channels 1 and 2 and channels 3 and 4 are close to zero in the first and second EMP, respectively. This means that the variation patterns of these channels can be decoupled by using the first two EMPs. As discussed later in the case study section, this property can help us study the condition of the forging machine.

Furthermore, the matrix of the first four eigenvectors, $\mathbf{E}_4 \in \Re^{700\times 4}$, was obtained by applying VPCA to the generated profile under scenario 1. Each eigenvector contains 175×4 data points, and each segment containing 175 data points corresponds to one profile channel. These eigenvectors are depicted in Fig. 3(b); each subplot represents one eigenvector and they are sorted in descending order of their relative importance from top to bottom. The relative importance c'_r can be calculated as $c'_r = S'_r / \sum_{r=1}^{4} S'_r$, where S'_r is the rth diagonal element of matrix $\mathbf{E}_4^{\mathrm{T}}\mathbf{X}\mathbf{X}\mathbf{E}_4$. These values are 0.3076, 0.3030, 0.1993, and 0.1901 for the four eigenvectors, respectively. Since all values of relative importance are large, all eigenvectors obtained from VPCA are plotted. As can be seen from the two top subplots of Fig. 3(b), the VPCA eigenvectors of profile channels 1 and 2 show a similar variation pattern to those obtained from UMPCA. However, as opposed to UMPCA, the relative importance values of eigenvectors 3 and 4 are large and reflect a significant variation pattern, as can be seen in Fig. 3(b). That is, the large variances of REs could not be completely captured by the two first sets of eigenvectors, and more eigenvectors are needed to fully characterize the variation pattern of multichannel profiles. This implies that UMPCA is more parsimonious than VPCA in terms of the number of features required to capture the majority of variations. This is because VPCA breaks the structure of the original data by reshaping them into vectors and loses potentially more compact or useful representations that can be obtained in the original form.

A similar analysis was carried out for the generated profile data under scenario 2 and the results are presented in Fig. 4. The relative importance values for UMPCA are 0.7905, 0.1496, 0.0461, and 0.0138. Therefore, eigenvectors corresponding to the two first EMPs are plotted in Fig. 4(a). In the first subplot in Fig. 4(a), the eigenvectors of channels 1 and 2 are overlapped, which indicates a strong positive correlation between two profile channels with the absolute correlation coefficient larger than 0.98 and p-value less the 0.0001. The eigenvectors of channels 3 and 4 show no variation pattern in the first EMP. However, the second subplot in Fig. 4(a) shows a strong negative correlation between profile channels 3 and 4 with an absolute correlation coefficient larger than 0.98 and p-value less the 0.0001 and no variation pattern in channels 1 and 2. Moreover, the relative importance of the first EMP is almost five times larger than that of the second EMP, which implies that variances in profile channels 1 and 2 are much larger than the

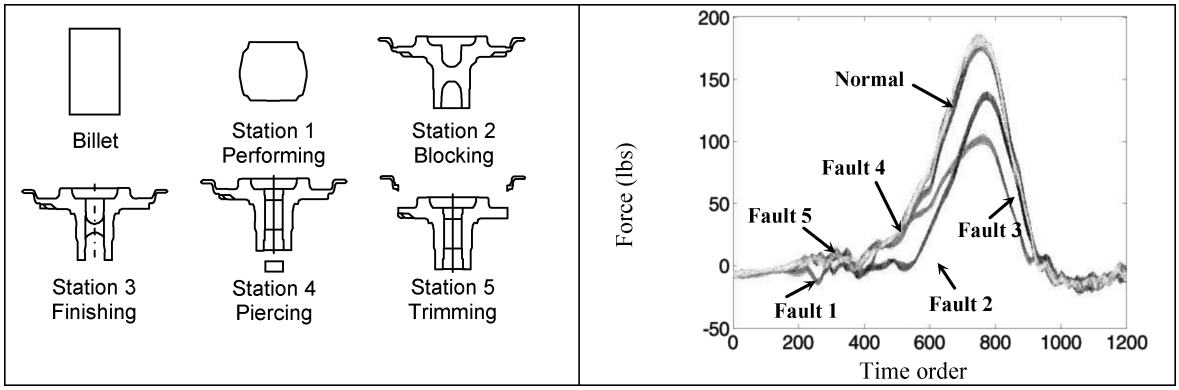

Fig. 5. (a) (left panel): Shape of workpieces at each operation and (b) (right panel): overlapping samples of aggregated tonnage profiles for normal and missing operations.

variances in profile channels 3 and 4. These results are exactly compatible with the data generation model, in which the profile data are generated so that channels 1 and 2 are highly positively correlated, channels 3 and 4 independent of channels 1 and 2 are highly negatively correlated, and the variances of channels 1 and 2 are five times larger than variances of channels 3 and 4. Additionally, the first and second EMPs characterize the variations of channels 1 and 2 and channels 3 and 4 separately, which could be useful in fault diagnosis.

Furthermore, VPCA was applied to the generated profile data in scenario 2. Relative importance values for VPCA are 0.4785, 0.2523, 0.2107, and 0.0585. The first three sets of eigenvectors are plotted in Fig. 4(b). Similar to UMPCA, the first subplots of Fig. 4(b) indicate a high positive correlation in channels 1 and 2 and no variation pattern in channels 3 and 4. However, as opposed to UMPCA, in the second and third sets of eigenvectors, only variation patterns of channels 1 and 2 are seen to be significant. In other words, the variations and interrelationship of channels 3 and 4 cannot be captured by VPCA. This is because in VPCA, the very large variations of channels 1 and 2 cannot be completely modeled by the first set of eigenvectors and are propagated in all sets of eigenvectors that can mask the variation patterns and interrelationship of other channels with smaller variances.

Based on the results obtained from the analysis of different simulation scenarios, it can be concluded that the UMPCA method is more efficient and precise than VPCA in summarizing and characterizing the variations in multichannel profiles.

4. Case study: variation characterization and fault diagnosis using multichannel tonnage profiles

In this section, we analyze multichannel tonnage profile data of a multi-operation forging process using both UMPCA and VPCA. In a multi-operation forging process, multiple dies work in a forging machine to produce a part. Each die performs one operation at each stroke as shown in Fig. 5(a). In this figure, intermediate workpieces after each operation of the selected forging process are shown. As described in the Introduction, there are four strain gauge sensors, one on each column of the press machine, that measure the force of the press uprights. Therefore, a four-channel profile is recorded for each stroke of the operation. These profiles provide rich information about the product quality and process conditions. Despite the previous research, which analyzed either the aggregated profile obtained from the summation of the four profile channels or each profile channel individually, we used UMPCA to examine these multichannel profiles, simultaneously.

In the four-channel profile data, each profile contains information about the force of the press machine during each stroke, which includes five different operations as shown in Fig. 5(a). Therefore, each profile can be divided into a few segments, which specify the working boundary of each operation. In each segment, only a few operations are active; that is, the force profile in each segment corresponds to active stations. Lei *et al*. (2010) developed a change-point detection method based on wavelets to determine segment boundaries. Based on their method, each tonnage profile can be divided into nine segments. Table 1 shows the time interval corresponding to each segment of a profile.

Table 1. Tonnage profile segments

	Segment								
	1	*2*	*3*	*4*	*5*	*6*	*7*	*8*	*9*
Time interval	[1,153]	[154,212]	[213,296]	[297,447]	[448,560]	[561,635]	[636,816]	[817,865]	[866,1200]

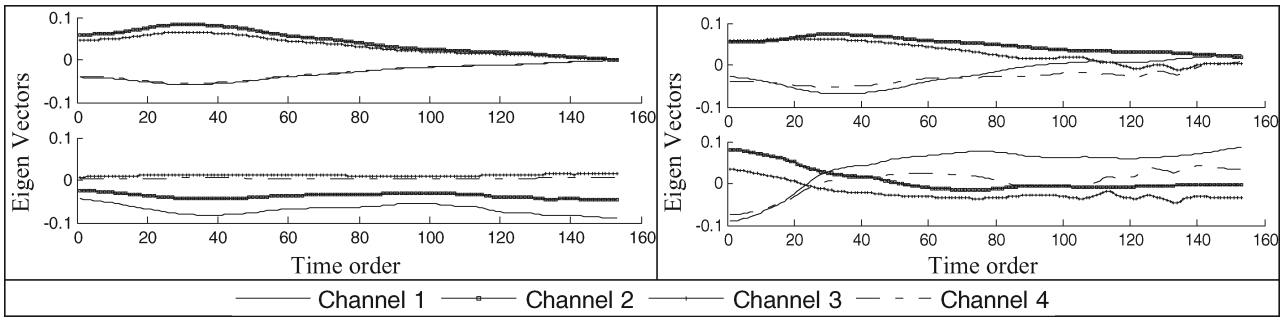

Fig. 6. UMPCA and VPCA results for segment 1: (a) (left panel): eigenvectors from UMPCA and (b): (right panel): eigenvectors from VPCA.

In this study, we consider one group of four-channel tonnage profiles under normal production conditions that consists of 306 samples and five fault groups of profiles under different missing part conditions, each of which consists of 69 samples. In each fault group, one part is missing in one operation of the forging process. The overlapping samples of aggregated tonnage profiles for normal and each fault group are depicted in Fig. 5(b). It should be noted that in terms of between-profile variability, the stationarity assumption (at least in a weak sense) is required for both VPCA and UMPCA modeling. In terms of within-profile variability, VPCA and UMPCA can also be applied if the stationarity assumption is violated, although in the latter case the noise within a profile may result in a lower performance of the approach. This means that de-noising is a very important step of the approach. In this article, prior to analyzing the multichannel tonnage profiles, each profile sample is de-noised using a wavelet-based soft-thresholding method (Donoho and Johnstone, 1995). There are two goals for this study. First, we are interested in characterizing the process variation associated with the press machine. For this purpose, we analyze segment 1 of tonnage profiles under normal production conditions. The second goal is to utilize the information of other segments of multichannel tonnage profiles for the purpose of fault detection and diagnosis.

In the first part of the case study, we apply UMPCA and VPCA to the first segment of the tonnage profiles obtained under normal conditions. This segment corresponds to the pre-operation stage in which the die starts moving toward parts to perform operations. Since there is no operation involved in this segment of the profiles, analyzing this segment data can provide us with useful information about the condition of the forging machine and clearance of the machine's die. Both UMPCA and VPCA were applied to profile data of segment 1. The eigentensors and eigenvectors obtained from UMPCA and VPCA are depicted in Figs. 6(a) and 6(b), respectively. The relative importance values for UMPCA are 0.8458, 0.1036, 0.0412, and 0.0094, whereas for VPCA these values are 0.7645, 0.1014, 0.0913, 0.0428. Only the first two important eigenvectors are shown in Fig. 6.

As can be seen from Fig. 6(a), the first EMP indicates that the variation patterns for channels 1 and 4 oppose those for channels 2 and 3. By reference to Fig. 1(a), it is clear that the sensors for channels 1 and 4 and for channels 2 and 3 are placed in the front and back side of the die, respectively. Therefore, the first EMP plot implies that the clearance between moving slides and press uprights may not be uniform or the upper die weight is not uniformly distributed over the upper moving bed, which causes the opposite movement direction for the front and back side of the upper dies. In other words, when the front side of the upper die moves upward, the back side moves downward, and *vice versa*. In the second EMP plot, the eigenvectors of channels 3 and 4 are almost zero, whereas the eigenvectors of channels 1 and 2 are non-zero. This implies that the movement variations in the right side of the die are larger than those in the left side of the die. Based on the relative importance index, the third and fourth EMP are negligible. On the other hand, as shown in Fig. 6(b), the eigenvectors obtained from VPCA are not as informative as the eigenvectors of UMPCA. Although the first set of eigenvectors obtained from VPCA is almost similar to those of UMPCA, the second set of eigenvectors is much different and indicates no clear result.

The goal of the second part of the case study is to utilize the UMPCA and classification methods for detecting strokes with missing parts and classifying their types. At first, to reduce the dimensions of the four-channel tonnage profiles, UMPCA was applied to the profile data under normal production. The resulting principal components $(\mathbf{y}_k(r) = \mathbf{V}_k \times_{l=1}^{2} \{\mathbf{u}_r^{(l)^{\mathrm{T}}}\}_{r=1}^{R})$ were considered as features to be used for further classification. The obtained eigentensors from the normal profile data were used to calculate the principal components and extract features from tonnage profiles of fault groups. Then, the extracted features were used to implement Bayesian classifiers (Hastie *et al*., 2009), which help not only detect the fault groups but to detect the type of missing part. As shown in Fig. 5(b), since the tonnage force for performing operations 2 and 3 is larger than the force of the other operations, the missing parts corresponding to these two operations can easily be

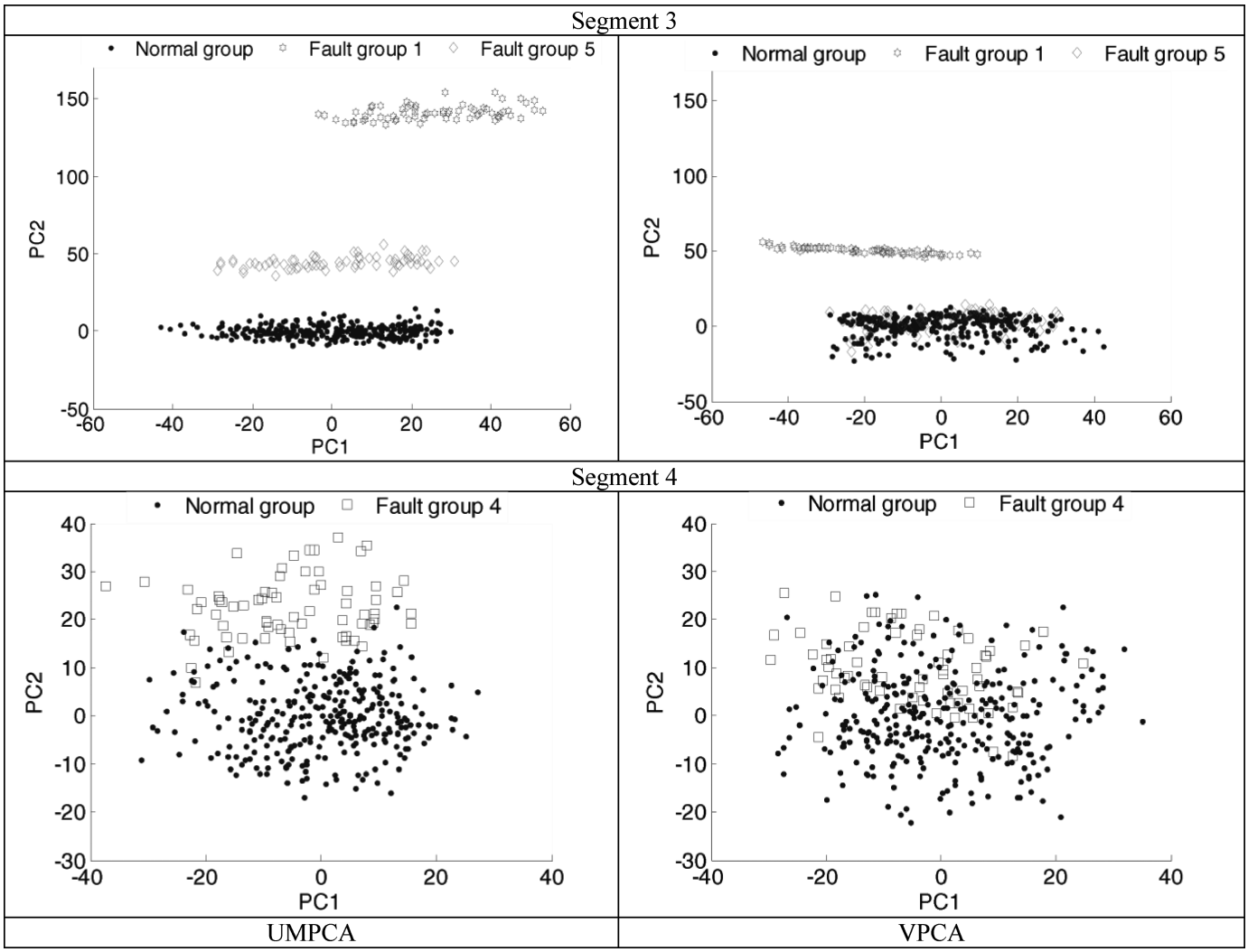

Fig. 7. Scatter plots across different fault groups for principal component extracted from UMPCA and VPCA methods using segments 3 and 4.

detected even by visual inspection of a profile. Therefore, we excluded these two faults from the analysis. For other operations, the difference in the exerted force of full operations and operations with missing part is so small that if the whole tonnage profile is used, we may not be able to detect the missing part operations. Therefore, for each fault group, we focused on a segment in which the corresponding operation was active. Segment 3 was selected for fault groups 1 and 5, and segment 4 was selected for fault group 4. In order to compare UMPCA with VPCA, the same analysis was repeated using VPCA and the results of two methods were compared.

Based on the relative importance index, the first two principal components of each method were selected as features for classification. The scatter plots of these principal components for normal and fault groups are plotted in Fig. 7.

As shown in Fig. 7, using both UMPCA and VPCA methods, samples in fault group 1 are completely separable from samples in the normal group. However, as can be implied from Fig. 5(b), detecting and classifying missing parts in fault groups 4 and 5 is more challenging since the overall shape of tonnage profiles for these fault groups is very similar to the profiles' shape for the normal group. Nevertheless, as can be seen in Fig. 7, using UMPCA, the samples in fault group 4 can be completely detected. Also, the extracted UMPCA features of fault group 5 are reasonably separable from those of the normal group. In contrast, because of the deficiencies of VPCA discussed earlier, the principal components obtained from VPCA are not correct features for separating fault samples in groups 4 and 5 from normal samples. The extracted features, shown in Fig. 7, were further used to construct Bayes classifiers. Let $\omega_i; i \in \{N, F_1, F_4, F_5\}$ denote the group of profile data, where N represents the normal group and F_1, F_4, and F_5 represent three fault groups. Based on the Bayes formula, the posterior probability for group i, $i \in \{N, F_1, F_4, F_5\}$,

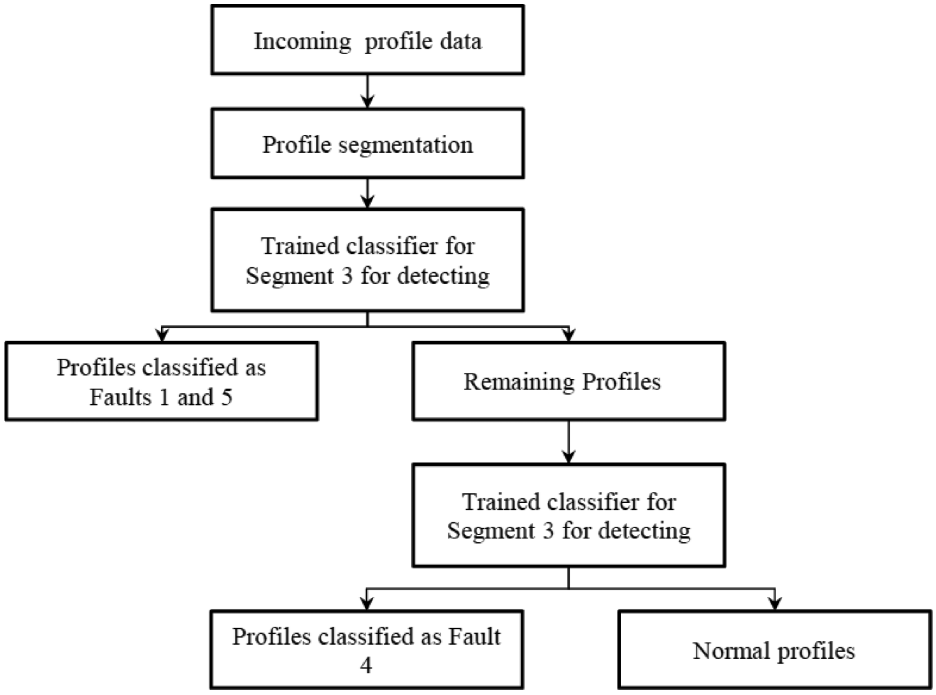

Fig. 8. Flow diagram of the developed procedure for detecting and classifying the missing parts in the multiple-operation forging process.

denoted by $\hat{P}(\omega_i|\mathbf{y})$ is calculated as follows:

$$\hat{P}(\omega_i|\mathbf{y}) = \hat{f}(\mathbf{y}|\omega_i)\hat{\pi}_i, \tag{6}$$

where $\mathbf{y}$ is the vector of extracted features (principal components), $\hat{f}(\mathbf{y}|\omega_i)$ and $\hat{\pi}_i$ respectively represent estimated normal likelihood functions and empirically estimated prior probabilities for group i. Since the principal components are linear combinations of the original variables, it is reasonable to assume that the principal components are normally distributed.

As shown in Fig. 7, fault groups 1 and 5 can be detected using segment 3, and fault group 4 can be separated using segment 4. Therefore, to effectively detect and classify fault groups, we used a hierarchical structure to develop the classification approach. The hierarchical classification procedure is shown in the flow diagram of Fig. 8. First, two Bayes classifiers were trained using segments 3 and 4 of the profile data. In online monitoring, when an incoming signal is recorded, principal component features are extracted for segments 3 and 4. At the first level of hierarchy, the trained classifier for segment 3 is used to detect fault groups 1 and 5. If the profile is classified as neither fault group 1 nor fault group 5, it proceeds to the second level of the hierarchy, in which they are classified as either fault group 1 or normal profiles.

To evaluate the performance of each classifier, a 10-fold cross-validation (Hastie *et al*., 2009) was used. Overall confusion matrices obtained from these classifiers are reported in Table 2 for both UMPCA and VPCA features. As expected, using both UMPCA and VPCA, fault group 1 can be accurately detected and classified. However, for fault groups 4 and 5, which are difficult faults to detect, the features provided by UMPCA lead to much better results than features obtained by VPCA. For fault 4, if UMPCA principal components are used, on average 92.75% of the missing parts can be correctly detected and classified, whereas this value for VPCA features is only 23.19%. Additionally, for fault 5, UMPCA features are able to accurately detect and classify all missing parts, whereas the features of VPCA are

Table 2. Confusion matrix of hierarchical Bayes classifiers for UMPCA and VPCA features obtained from 10-fold cross-validation

	Classified as			
	Normal	*Fault 1*	*Fault 4*	*Fault 5*
		UMPCA		
Actual				
Normal	298	0	8	0
Fault 1	0	69	0	0
Fault 4	5	0	64	0
Fault 5	0	0	0	69
		VPCA		
Actual				
Normal	291	0	15	0
Fault 1	0	69	0	0
Fault 4	53	0	16	0
Fault 5	69	0	0	0

not able to detect this type of fault. In terms of false alarm rate, the UMPCA features with a 2.61% error rate are also slightly better than VPCA features with a 4.90% error rate.

5. Conclusions

In this article, based on UMPCA, we proposed a method for effective analysis of multichannel profiles. In contrast with existing methods, the proposed method not only utilizes information on each profile channel but takes the interrelationship among different profile channels into consideration. A simulation study was conducted to evaluate the performance of the proposed method and show its performance superiority over VPCA. The results showed that as opposed to UMPCA, VPCA fails to fully characterize the profiles' variations and their interrelationships. We also applied both UMPCA and VPCA to a real case study of a forging process for the purpose of variation characterization of a press machine and fault diagnosis. The results indicated that UMPCA outperforms VPCA in not only detecting the faulty operations with missing parts but also in classifying the type of faults. Using UMPCA features, the overall error of the trained classifier is 2.53%, whereas this error for VPCA is 26.71%, which implies the superiority of UMPCA over VPCA.

In this article, we considered the case of multichannel homogenous profile data, where all sensors measure the same variable. However, another important and challenging problem is the analysis of multi-sensor heterogeneous profile data, in which various sensors measures different variables. The problem of analyzing such profile data using UMPCA for the purpose of data fusion, monitoring, and fault detection can be considered as a potential topic for future research. Analysis of designed experiments, in which the response variable is represented by multichannel profiles, is an interesting and challenging topic that can be pursued in the future.

References

Basir, O. and Yuan, X. (2007) Engine fault diagnosis based on multi-sensor information fusion using Dempster–Shafer evidence theory. *Information Fusion*, **8**, 379–386.

Bharati, M.H., Liu, J.J. and MacGregor, J.F. (2004) Image texture analysis: methods and comparisons. *Chemometrics and Intelligent Laboratory Systems*, **72**, 57–71.

Bharati, M.H. and MacGregor, J.F. (1998) Multivariate image analysis for real-time process monitoring and control. *Industrial and Engineering Chemistry Research*, **37**, 4715–4724.

Colosimo, B.M., Pacella, M. and Semeraro, Q. (2008) Statistical process control for geometric specifications: on the monitoring of roundness profiles. *Journal of Quality Technology*, **40**, 1–18.

Demidenko, E. (2004) *Mixed Models: Theory and Applications*, Wiley, New York, NY.

Ding, Y., Zeng, L. and Zhou, S. (2006) Phase I analysis for monitoring nonlinear profiles in manufacturing processes. *Journal of Quality Technology*, **38**, 199–216.

Donoho, D.L. and Johnstone, I.M. (1995) Adapting to unknown smoothness via wavelet shrinkage. *Journal of American Statistical Association*, **90**, 1200–1224.

Gao, Y. and Durrant-Whyte, H.F. (1994) Multi-sensor fault detection and diagnosis using combined qualitative and quantitative techniques, in *Proceedings of the IEEE International Conference on Multisensor Fusion and Integration for Intelligent Systems*, IEEE Press, Piscataway, NJ, pp. 43–50.

Gardner, M., Lu, J., Gyurcsik, R., Wortman, J., Hornung, B., Heinisch, H., Rying, E., Rao, S., Davis, J. and Mozumder, P. (1997) Equipment fault detection using spatial signatures. *IEEE Transaction on Components, Packaging, and Manufacturing Technology, Part C*, **20**, 294–303.

Gupta, S., Montgomery, D.C. and Woodall, W.H. (2006) Performance evaluation of two methods for online monitoring of linear calibration profiles. *International Journal of Production Research*, **44**, 1927–1942.

Hastie, T., Tibshirani, R. and Friedman, J. (2009) *The Elements of Statistical Learning: Prediction, Inference and Data Mining*, Springer Verlag, New York, NY.

Jensen, W.A. and Birch, J.B. (2009) Profile monitoring via nonlinear mixed models. *Journal of Quality Technology*, **41**, 18–34.

Jensen, W.A., Birch, J.B. and Woodall, W.H. (2008) Monitoring correlation within linear profiles using mixed models. *Journal of Quality Technology*, **40**, 167–183.

Jin, J. and Shi, J. (2001) Automatic feature extraction of waveform signals for in-process diagnostic performance improvement. *Journal of Intelligent Manufacturing*, **12**, 257–268.

Jolliffe, I.T. (2002) *Principal Component Analysis*, Springer, New York, NY.

Jung, U., Jeong, M.K. and Lu, J.C. (2006a) Data reduction for multiple functional data with class information. *International Journal of Production Research*, **44**(14), 2695–2710.

Jung, U., Jeong, M.K. and Lu, J.C. (2006b) A vertical-energy-thresholding procedure for data reduction with multiple complex curves. *IEEE Transactions on Systems, Man, Cybernetics, Part B*, **36**(5), 1128–1138.

Kang, L. and Albin, S.L. (2000) On-line monitoring when the process yields a linear profile. *Journal of Quality Technology*, **32**, 418–426.

Kim, J., Huang, Q., Shi, J. and Chang, T.-S. (2006) Online multi-channel forging tonnage monitoring and fault pattern discrimination using principal curve. *ASME Transactions, Journal of Manufacturing Science and Engineering*, **128**, 944–950.

Kim, K., Mahmoud, M.A. and Woodall, W.H. (2003) On the monitoring of linear profiles. *Journal of Quality Technology*, **35**, 317–328.

Kolda, T.G. (2001) Orthogonal tensor decompositions. *SIAM Journal of Matrix Analysis and Applications*, **23**, 243–255.

Lathauwer, L.D., Moor, B.D. and Vandewalle, J. (2000a) A multilinear singular value decomposition. *SIAM Journal of Matrix Analysis and Applications*, **21**, 1253–1278.

Lathauwer, L.D., Moor, B.D. and Vandewalle, J. (2000b) On the best rank-1 and rank-(R_1, R_2, ... , R_N) approximation of higher-order tensors. *SIAM Journal of Matrix Analysis and Applications*, **21**, 1324–1342.

Lei, Y., Zhang, Z. and Jin, J. (2010) Automatic tonnage monitoring for missing part detection in multi-operation forging processes. *ASME Transactions, Journal of Manufacturing Science and Engineering*, **132**, 051010-1–10.

Lu, H., Plataniotis, K.N. and Venetsanopoulos, A.N. (2008) MPCA: multilinear principal component analysis of tensor objects. *IEEE Transactions on Neural Networks*, **19**, 18–39.

Lu, H., Plataniotis K.N. and Venetsanopoulos, A.N. (2009) Uncorrelated multilinear principal component analysis for unsupervised multilinear subspace learning. *IEEE Transactions on Neural Networks*, **20**, 1820–1836.

Mahmoud, M.A., Parker, P.A., Woodall, W.H. and Hawkins, D.M. (2007) A change point method for linear profile data. *Quality and Reliability Engineering International*, **23**, 247–268.

Mahmoud, M.A. and Woodall, W.H. (2004) Phase I analysis of linear profiles with calibration applications. *Technometrics*, **46**, 380–391.

Moroni, G. and Pacella, M. (2008) An approach based on process signature modeling for roundness evaluation of manufactured items. *ASME Transactions, Journal of Computing and Information Science in Engineering*, **8**, 021003-1-10.

Mosallaei, M., Salahshoor, K. and Bayat, M. (2008) Centralized and decentralized process and sensor fault monitoring using data fusion based on adaptive extended Kalman filter algorithm. *Measurement Journal*, **41**, 1059–1076.

Mosesova, S.A., Chipman, H.A., MacKay, R.J. and Steiner, S.H. (2006) Profile monitoring using mixed-effects models. Technical report RR-06-06, University of Waterloo, Canada.

Paynabar, K. and Jin, J. (2011) Characterization of nonlinear profiles variations using mixed-effect models and wavelets. *IIE Transactions on Quality and Reliability Engineering*, **43**, 275–290.

Paynabar, K., Jin, J., Agapiou, J. and Deeds, P. (2012) Robust leak tests for transmission systems using nonlinear mixed-effect models. *Journal of Quality Technology*, **43**, 275–290.

Qiu, P., Zou, C. and Wang, Z. (2010) Nonparametric profile monitoring by mixed effects modeling. *Technometrics*, **52**, 265–277.

Quan, R., Quan, S.H., Huang, L. and Xie, C.J. (2010) Fault diagnosis and fault-tolerant control for multi-sensor of fuel cell system. *Journal of Computational Information Systems*, **6**, 3703–3711.

Walker, E. and Wright, S. (2002) Comparing curves using additive models. *Journal of Quality Technology*, **34**, 118–129.

Williams, J.D., Woodall, W.H. and Birch, J.B. (2007) Phase I analysis of nonlinear product and process quality profiles. *Quality and Reliability Engineering International*, **23**, 925–941.

Ye, J., Janardan, R. and Li, Q. (2004) GPCA: an efficient dimension reduction scheme for image compression and retrieval, in *Proceedings of the 10th ACM SIGKDD International Conference on Knowledge Discovery and Data Mining*, pp. 354–363.

Zou, C., Qiu, P. and Hawkins, D. (2009) Nonparametric control chart for monitoring profiles using change point formulation and adaptive smoothing. *Statistica Sinica*, **19**, 1337–1357.

Zou, C., Tsung, F. and Wang, Z. (2008) Monitoring profiles based on nonparametric regression models. *Technometrics*, **50**, 512–526.

Zou, C., Zhang, Y. and Wang, Z. (2006) A control chart based on a change-point model for monitoring profiles. *IIE Transactions - Quality and Reliability Engineering*, **38**, 1093–1103.

Biographies

Kamran Paynabar is an Assistant Professor in the H. Milton Stewart School of Industrial and Systems Engineering at Georgia Tech. He received his B.Sc. and M.Sc. in Industrial Engineering from Iran University of Science and Technology and Azad University in 2002 and 2004, respectively, and his Ph.D. in Industrial and Operations Engineering from the University of Michigan in 2012. He also holds an M.A. in Statistics from the University of Michigan. His research interests include data fusion for multi-stream waveform signals and functional data, engineering-driven statistical modeling, sensor selection in distributed sensing networks, probabilistic graphical models, and statistical learning with applications in manufacturing and healthcare systems. He is the recipient of the INFORMS Data Mining Best Student Paper Award, the Best Application Paper Award from *IIE Transactions*, and the Wilson Prize for the Best Student Paper in Manufacturing. He is a member of ASQ, IIE, and INFORMS.

Jionghua (Judy) Jin is a Professor in the Department of Industrial and Operations Engineering at the University of Michigan. She received her Ph.D. degree from the University of Michigan in 1999. Her recent research focuses on data fusion methodology development for improving complex system operations, which includes variation reduction, condition monitoring and fault diagnosis, process control, knowledge discovery, and decision making. Her research emphasizes an integration of applied statistics, signal processing, reliability, system control, and decision-making theory. She has received a number of awards including the NSF CAREER Award in 2002 and the PECASE Award in 2004, and eight Best Paper Awards during 2005–2012. She is a Fellow of ASME and a member of ASQ, IEEE, IIE, INFORMS, and SME.

Massimo Pacella is an Assistant Professor in the Department of Engineering for Innovation at the University of Salento, Lecce, Italy, where he teaches statistical process control and process improvement. In 2003, he received his Ph.D. degree in Manufacturing and Production Systems from the University Polytechnic of Milan, Italy. His major research interests are in signal processing, manufacturing process control and coordinate metrology, including the development of artificial intelligence techniques and methods of applied statistics. Based on his research achievements, he was awarded a Fulbright Fellowship in 2009. He is member of the Italian Association for Manufacturing (AITeM).